Cancer Chemother Pharmacol (2004) 54: 449–458
DOI 10.1007/s00280-004-0833-y

ORIGINAL ARTICLE

Dashnamoorthy Ravi · Kumuda C. Das

Redox-cycling of anthracyclines by thioredoxin system: increased superoxide generation and DNA damage

Received: 22 November 2003 / Accepted: 31 March 2004 / Published online: 28 July 2004

Abstract Anthracyclines such as doxorubicin and daunomycin undergo bioreductive activation by redox-cycling, and this is associated with generation of reactive oxygen species. Toxicity of anthracyclines is attributed to DNA intercalation by an anthracycline semiquinone radical that is generated via redox-cycling. Flavoprotein enzymes catalyze the bioreductive activation of anthracyclines. Thioredoxin reductase (TR), which is also a flavoprotein enzyme, participates in bioreductive activation of anthracyclines. In the present study we showed that addition of *E. coli* thioredoxin (Trx) enhances the rate of superoxide production by *E. coli* TR in the presence of anthracyclines. The superoxide generated in this redox-cycling process induced DNA damage as determined by an in vitro plasmid DNA damage assay. In addition, Trx-SH enhanced the activity of cytochrome P450 reductase and the redox-cycling of anthracyclines independently of NADPH. Furthermore, when A549 cells were incubated with *E. coli* Trx followed by doxorubicin treatment, increased levels of ROS generation were observed. Taken together, these results show a novel property of the Trx system in bioreductive activation of anthracyclines.

Keywords Redox-cycling · Anthracyclines · Thioredoxin · DNA damage

Introduction

Thioredoxin (Trx) and thioredoxin reductase (TR) constitute a ubiquitous redox system found in both prokaryotic and eukaryotic organisms. The biological role of TR is to transfer reducing equivalents from NADPH to various oxidized substrates while Trx is the major substrate. *Escherichia coli* TR is a homodimer comprising 35 kDa subunits and *E. coli* Trx is a 12 kDa protein [1] with two redox-active cysteine residues at positions 32 and 35. The active site of Trx is well conserved in both prokaryotic and eukaryotic systems. The two half cysteines at the active site of oxidized Trx are reduced by TR in a NADPH-dependant reaction. The reduced form of Trx, in turn, reduces several other proteins that are involved in DNA synthesis, signal transduction, and protein folding [1, 2]. Furthermore, reduced Trx is also an electron donor for Trx peroxidases that remove peroxides [3]. We have previously shown that Trx induces manganese superoxide dismutase (MnSOD) expression [4]. Furthermore, although Trx has been found to be a scavenger of hydroxyl radical and a quencher of singlet oxygen, it does not scavenge $O_2^{\bullet -}$ [5]. The mammalian Trx system has been shown to protect cells and tissues under various oxidative stress conditions [6]. Previous studies using mammalian TR have shown that doxorubicin is a substrate for mammalian TR. However, doxorubicin has also been shown to inhibit mammalian TR activity in an irreversible manner [7]. Additionally, although Trx was found to protect cells against H_2O_2-induced apoptosis, it does not protect against doxorubicin-induced apoptosis [8].

Anthracycline antibiotics are widely used in anticancer chemotherapy, and are quinone-based drugs, which undergo redox-cycling process [9]. The redox-cycling process involves the quinone moiety of anthracycline, which accepts an electron in the reaction catalyzed by flavoprotein enzymes and converted into semiquinone form. The semiquinone radical in turn reacts with molecular oxygen to produce the superoxide radical ($O_2^{\bullet -}$) and regenerates the quinone completing the redox cycle. Flavoprotein enzymes, such as cytochrome P450 reductase (CPR), are known to be involved in the redox-cycling process of anthracyclines [8]. Redox-cycling of anthracyclines results in damage to the DNA that activates p53-induced apoptosis of cancer cells. Thus, redox-cycling is a fundamental process that is

D. Ravi · K. C. Das (✉)
Department of Molecular Biology, University of Texas Health Center at Tyler, 11937 US Hwy 271, Tyler, TX 75708, USA
E-mail: kumuda.das@uthct.edu
Tel.: +1-903-8777418
Fax: +1-903-8777675

important for the effectiveness of anthracycline chemotherapy.

While determining the protective effect of the Trx system against anthracycline-mediated DNA damage, we have observed that Trx cannot prevent anthracycline-induced plasmid DNA damage; rather increased DNA damage has been observed in the presence of the Trx system. Since anthracycline redox-cycling generates reactive oxygen species (ROS) known to induce DNA damage, we sought to determine the role of Trx system in anthracycline redox-cycling. Thus, the objective of this study was to evaluate whether reduced Trx could increase the redox-cycling of anthracyclines. Additionally, we also sought to determine whether Trx-enriched cells were more susceptible to apoptotic death in the presence of anthracyclines.

In the study reported here, we demonstrated that the *E. coli* Trx system enhanced the redox-cycling of anthracyclines, and thus increased the generation of $O_2^{\bullet-}$. Additionally, reduced Trx could also act as an electron donor for CPR. Furthermore, we also showed that *E. coli* Trx enhanced the redox-cycling of anthracyclines in lung adenocarcinoma A549 cells.

Materials and methods

Reagents

Escherichia coli Trx was obtained from Promega (Madison, Wis.). *Escherichia coli* TR was obtained from American Diagnostica (Greenwich, Ct.). Cytochrome *c* (partially acetylated), daunomycin, doxorubicin, NADPH, NADPH CPR (rabbit liver), and superoxide dismutase (SOD) were purchased from Sigma Chemicals (St Louis, Mo.).

Superoxide detection by cytochrome *c* reduction assay

Superoxide ($O_2^{\bullet-}$) generated in the process of redox-cycling was detected by the SOD-inhibitable rate of ferricytochrome *c* reduction [5]. The reaction mixture contained 0.05 *M* potassium phosphate buffer (pH 7.78), 1 m*M* EDTA, 10 μ*M* cytochrome *c*, and 200 μ*M* NADPH. For detection of SOD-inhibitable rate of reduction, 1–5 U SOD was included in the assay; daunomycin or doxorubicin was used at a final concentration of 10 μ*M*, standardized for optimal detection of $O_2^{\bullet-}$ by this assay. The rate of reduction of cytochrome *c* was measured at 550 nm for 0–15 min using a Shimadzu UV-1601PC in kinetic mode with intervals assigned by the software. The reaction blank contained potassium phosphate buffer, cytochrome *c*, and NADPH with or without SOD, and 0.35 μg/ml TR and/or Trx was included in the controls. All reactions were performed in triplicate. The rate of change in optical density ($OD \times 10^{-3}$ per minute) was used to determine the rate of $O_2^{\bullet-}$ generation using an extinction coefficient of 19,600 M^{-1} min^{-1} for reduced ferricytochrome *c* at 550 nm [10]. The microtiter assay was performed in a volume of 250 μl, where the concentrations of reactants were similar to those described for the spectrophotometric assay (using spectramax 190 molecular Devices). The rate of reduction of ferricytochrome *c*, as well as disappearance of NADPH were measured at 550 and 340 nm simultaneously. The CPR-mediated SOD-inhibitable rate of $O_2^{\bullet-}$ generation was determined with reduced Trx as an electron donor using a similar method to that described above along with cytochrome P450 reductase (0.04 U). Statistical analysis was performed using InStat 6.01 software (InStat, San Diego, Calif.).

Preparation of reduced Trx

Reduced Trx was prepared by incubating 850 μ*M* *E. coli* Trx with 2 m*M* dithiothreitol (DTT) for 30 min at room temperature as described previously [4]. Excess DTT was removed using Biospin-6 desalting columns (Biorad, Hercules, Calif.) equilibrated with 10 m*M* Tris, pH 7.0. The concentration of Trx-SH was determined using molar extinction coefficient of 13,700 at A_{280} [11].

Cytochrome P450 reductase activity assay

CPR activity was determined as described previously [12] with the following modifications. The reaction mixture contained 0.05 *M* potassium phosphate buffer (pH 7.7), 0.04 U of purified rabbit liver CPR enzyme, and 50 μ*M* cytochrome *c*. The reaction was initiated by the addition of 11.2 μ*M* of Trx-SH or Trx-S_2, and was followed for 0–5 min at 550 nm (Shimadzu UV-1601PC).

Plasmid DNA-damage assay

Plasmid DNA (1 μg, pBL-CAT6) was incubated with 10 μ*M* doxorubicin in potassium phosphate buffer (0.05 *M*, pH 7.8) containing 0.35 μg/ml TR or 3.2 μ*M* Trx, and 200 μ*M* NADPH with or without 2 U SOD. The control plasmid was incubated with NADPH. The reaction mixture was incubated for 12 h for optimal yield of nicks, as standardized for our assay. Following incubation, the reaction mixture was resuspended in 1× DNA gel loading buffer (6× gel loading buffer: 0.25% each bromophenol blue and xylene cyanol FF and 30% glycerol in water), and analyzed by 1% agarose gel electrophoresis using a standard protocol. The gel was stained with ethidium bromide and photographed using a Biorad gel documentation system (Biorad, Hercules, Calif.).

Carboxymethylation of Trx

In order to determine the role of Trx in the redox-cycling of anthracyclines, the redox status of Trx was determined by carboxymethylation at the end of a redox-cycling reaction. The reaction mixture contained 0.05 *M* potassium phosphate buffer (pH 7.78), 1 m*M* EDTA, and 200 μ*M* NADPH with or without 1–5 U SOD and with or without 10 μ*M* doxorubicin. TR and Trx were used at 0.35 μg/ml and 3.2 μ*M* final concentrations, respectively. Carboxymethylation was performed after 30 min of reaction time as described in our previous studies [4]. An equal volume of carboxymethylation buffer (0.1 *M* Tris, pH 8.8, 12 mg/ml iodoacetic acid, 3 m*M* EDTA, 7 *M* guanidine hydrochloride, and 0.5% Triton X-100, equilibrated with nitrogen for 1 h) was added followed by incubation at 37°C in the dark for 45 min. Following incubation, excess reagent was removed using a Sephadex G-25 spin column, and the eluted protein was used for Western blot detection of Trx.

Western analysis of Trx redox state

Equal amounts of protein were fractionated along with standards of *E. coli* Trx-SH and Trx-S_2 on a 15% native polyacrylamide gel. The protein was transferred to PVDF membrane using a miniprotein transblot apparatus (Bio-Rad). The PVDF membrane was washed and incubated with mouse anti-*E. coli* Trx IgG (MBL, Nagoya, Japan). After washing, the blots were incubated with anti-mouse IgG–horseradish peroxidase conjugate for 1 h at room temperature. Binding of secondary antibody was detected using an enhanced chemiluminescence (ECL Plus) detection system (Amersham Pharmacia Biotech, Piscataway, N.J.). The Western blots were quantified using densitometric analysis software (NIH Image 1.61).

Uptake of *E. coli* Trx by A549 cells; detection by immunofluorescence

Cells (25,000) were seeded in chambered glass slides, and were allowed to attach overnight and then incubated with *E. coli* Trx (Promega, Madison, Wis.) to a final concentration of 32 μ*M* for 16 h. Cells were washed twice with PBS, fixed in 4% paraformaldehyde for 30 min and washed again with PBS. Blocking of nonspecific binding was performed by incubating the fixed cells in 3% bovine serum albumin (BSA) for 1 h followed by overnight incubation with mouse anti-*E. coli* Trx IgG (MBL, Nagoya, Japan) at 4°C. Binding of the primary antibody was detected using Alexa Fluor 488 anti-mouse IgG (Molecular Probes, Eugene, Ore.), and was analyzed with a Nikon microscope attached to a Perkin-Elmer laser confocal scanning unit. Images were recorded using *Z*-axis controlled in 1 μ*M* steps.

TUNEL assay

DNA strand breaks were identified based on terminal deoxynucleotidyl transferase-mediated nick end-labeling (TUNEL) of 3′-OH termini using the fluorescein-dUTP technique (Roche Biochemicals, Indianapolis, Ind.). For this assay A549 cells were seeded to a final density of 25,000 cells per well, and were allowed to adhere overnight in chambered glass slides (Nunc). Cells were then preincubated with *E. coli* Trx for 16 h, followed by treatment with appropriate concentrations of drugs for 4 h. The medium was removed, and cells were washed twice with PBS containing 1% BSA and fixed in 4% paraformaldehyde for 30 min, and rinsed with PBS containing 1% BSA. Cells were then permeabilized with 0.1% Triton X-100 in 0.1% sodium citrate for 2 min on ice, and washed twice with PBS containing 1% BSA. The labeling reaction was performed using terminal deoxynucleotidyl transferase and FITC-labeled dUTP along with other nucleotides for 60 min in the dark at 37°C in a humidified chamber. Cells were washed with PBS/1% BSA and mounted, and the incorporated fluorescein-dUTP was analyzed using a Nikon microscope attached to a Perkin-Elmer laser confocal scanning unit at 488 nm. Images were captured using Ultraview software (Perkin-Elmer) with correction for background fluorescence emitted by anthracyclines.

In situ detection of ROS by fluorescent probe dicarboxyfluorescein-diacetate (DCF-DA)

A549 cells were grown in chambered glass slides (Nunc) to a final density of 25,000 cells per well. Cells were then preincubated with *E. coli* Trx for 16 h, followed by incubation with 20 μ*M* DCF-DA (Sigma, St Louis, Mo.) in 20 m*M* HEPES in PBS containing BSA (5 mg/ml) at 37°C for 30 min followed by washing with PBS buffer. Appropriate concentrations of drug were added, and green fluorescence was measured at specific times using a Nikon microscope attached to a Perkin-Elmer laser confocal scanning unit with a laser beam wavelength of 488 nm for 300 s. All treatments were time-matched to avoid leakage of DCF-DA, and the settings were optimized for controlling nonspecific excitation of DCF-DA by the laser, and corrected for background fluorescence by anthracyclines. The results were analyzed using Ultraview software (Perkin-Elmer), and plotted as mean fluorescent intensity per 100 cells vs duration of incubation.

Nuclear extract preparation

Nuclear extract was prepared as described previously [13]. Briefly, cells were washed in ice-cold PBS and harvested in 2 ml ice-cold PBS by centrifugation, followed by removal of PBS. The cell pellet was resuspended in 400 μl buffer A (10 m*M* HEPES, pH 7.8,

10 m*M* KCl, 0.1 m*M* EDTA, 1 m*M* dithiothreitol, 1 m*M* phenylmethylsulfonyl fluoride (PMSF), and 50 μg/ml of leupeptin and anti-pain) by gentle pipetting. Cells were allowed to swell on ice for 15 min followed by addition of 25 μl 10% Nonidet-P40 and vortexed at full speed for 10 s. The homogenate was centrifuged for 30 s at 14,000 rpm. The nuclear pellet was resuspended in buffer C (20 m*M* HEPES, pH 7.8, 0.42 *M* NaCl, 5 m*M* EDTA, 1 m*M* dithiothreitol, 1 m*M* PMSF in 10% v/v glycerol) and the tubes rocked gently at 4°C for 30 min on a shaking platform. The extract was then centrifuged at 14,000 rpm for 25 min, and the supernatant was saved as nuclear extract at −70°C for further experiments. Protein was quantified using the Bradford protein assay (Biorad).

p53 electrophoretic mobility shift assay (EMSA)

For the EMSA the p53 consensus oligonucleotide was obtained from Genosys (5′-GGCATGTCCGGG-CATGTCC-3′) and end-labeled using T4 polynucleotide kinase (New England Biolabs, Beverly, Mass.) and [γ-^{32}P] ATP (Perkin-Elmer, Boston, Mass.) in the 10× kinase buffer supplied with the enzyme. Nuclear protein (10 μg) was preincubated in 5 μl 5× binding buffer (20% glycerol, 5 m*M* $MgCl_2$, 5 m*M* EDTA, 5 m*M* DTT, 500 m*M* NaCl, 50 m*M* Tris-HCl, 0.4 mg/ml calf thymus DNA), 200 ng anti-p53 pAb421 and 2 μg poly-dIdC for 15 min followed by binding with labeled oligonucleotide for 30 min. The nuclear protein was separated by electrophoresis using 4% native polyacrylamide gel and 0.25× of TBE (Tris-borate-EDTA) as running buffer.

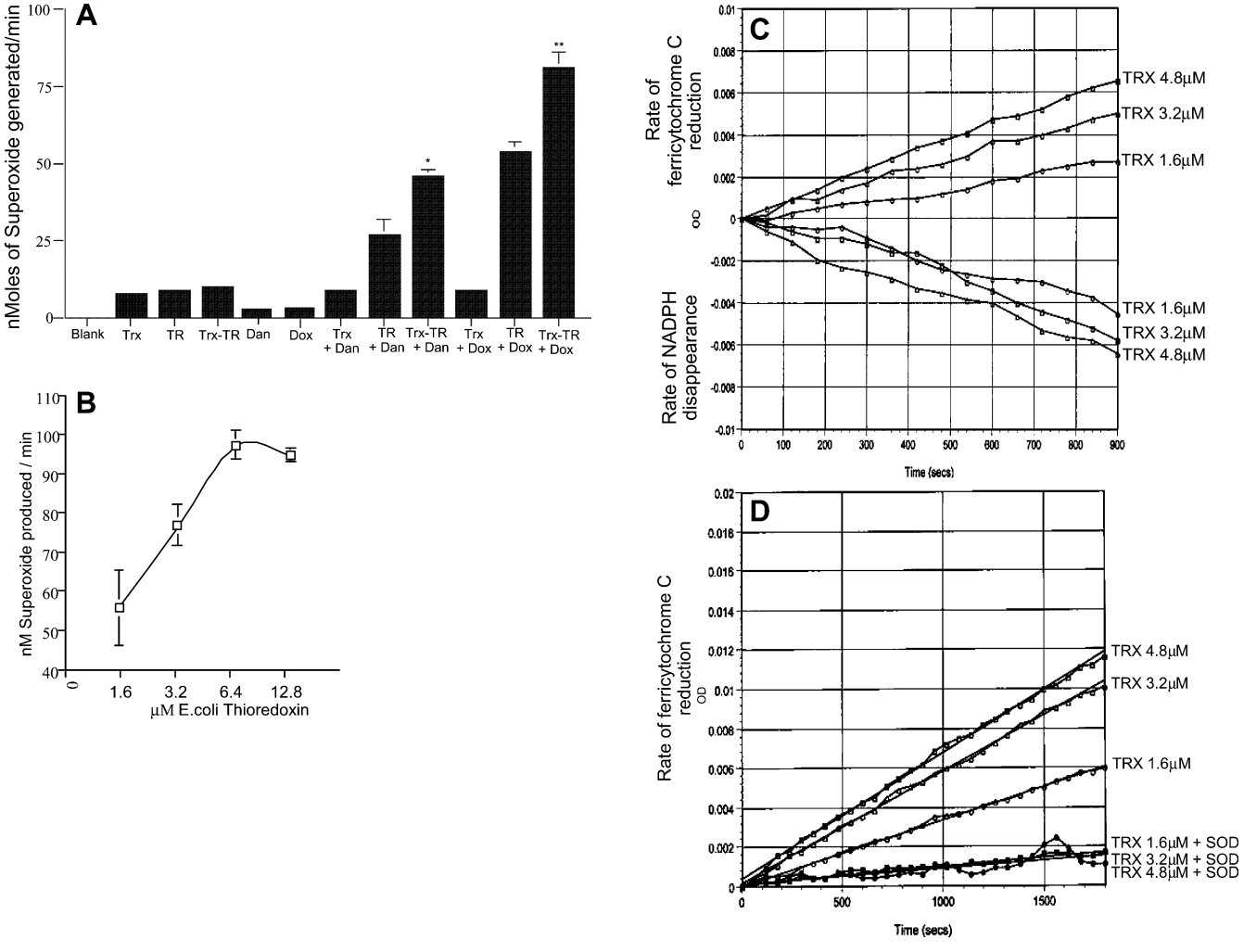

Fig. 1 **a** Anthracyclines generate $O_2^{-\bullet}$ with the Trx system. $O_2^{-\bullet}$ generation was determined by the SOD-inhibitable reduction of ferricytochrome *c* as described in Materials and methods. The reaction mixture contained the following: *lane 1* NADPH blank, *lane 2* 3.2 μ*M* Trx, *lane 3* 0.35 μg/ml TR, *lane 4* 3.2 μ*M* Trx and 0.35 μg/ml TR, *lane 5* 10 μ*M* daunomycin, *lane 6* 10 μ*M* doxorubicin, *lanes 7–12* the concentrations of Trx and TR were the same as those in *lane 2* and *lane 3* and the drug concentration was 10 μ*M*. **P* < 0.05 vs *lane 8*, ***P* < 0.05 vs *lane 11*. **b–d** Effect of Trx concentration on $O_2^{\bullet-}$ generation with doxorubicin: **b** increasing the concentration of Trx from 1.6 to 12.8 μ*M* with constant TR (0.35 μg) and 10 μ*M* doxorubicin enhanced $O_2^{\bullet-}$ generation in a concentration-dependent manner; **c** simultaneous detection of reduction of ferricytochrome *c* and disappearance of NADPH in 250 μl reactions adapted for a microplate containing increasing concentrations of Trx from 1.6 to 4.8 μ*M* with constant TR (0.35 μg/ml) and 10 μ*M* doxorubicin; **d** reduction of ferricytochrome *c* in the above reactions with SOD (5 U/ml)

The gels were dried and exposed to Kodak Biomax X-ray film overnight.

Results

Anthracyclines generate superoxide anion with Trx system

The addition of daunomycin or doxorubicin to the Trx system enhanced $O_2^{\bullet-}$ generation as detected by the SOD-inhibitable rate of reduction of ferricytochrome *c*. The Trx-TR system did not induce significant levels of SOD-inhibitable ferricytochrome *c* reduction (Fig. 1a, lane 4). Daunomycin or doxorubicin alone also did not induce significant levels of SOD-inhibitable ferricytochrome *c* reduction (Fig. 1a, lanes 5 and 6). However, the TR-Trx system generated significantly higher levels of $O_2^{\bullet-}$ with daunomycin or doxorubicin. The TR-Trx system showed higher levels of superoxide generation in the presence of doxorubicin than with daunomycin (Fig. 1a, lanes 8–12). Increasing the concentration of Trx from 1.6 to 6.4 μ*M* in reactions with 0.35 μg/ml TR resulted in a proportional increase in the rate of $O_2^{\bullet-}$ generation with doxorubicin (Fig. 1b). Further increases in Trx concentration did not increase the rate of $O_2^{\bullet-}$ generation, indicating that a saturation concentration of Trx had been reached (Fig. 1b). Reactions were modified to adapt simultaneous determination of the rates of reduction of ferricytochrome *c* and the disappearance of NADPH in a microtiter assay containing 1.6–4.8 μ*M* Trx with 0.35 μg/ml TR and 10 μ*M* doxorubicin. A proportional increase in the rate of ferricytochrome *c* reduction and disappearance of NADPH was observed (Fig. 1c). The addition of SOD to these reactions inhibited the rate of ferricytochrome *c* reduction (Fig. 1d).

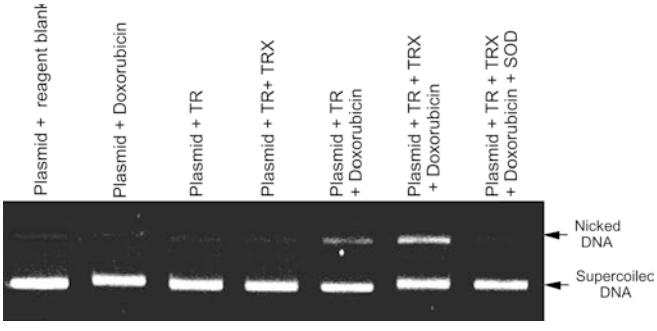

Fig. 2 Redox-cycling of anthracyclines by the Trx system induces nicks in plasmid DNA mediated by $O_2^{\bullet-}$. Plasmid DNA pBL-CAT6 incubated with doxorubicin and the Trx system for 2 h and analyzed by agarose gel electrophoresis as described in Materials and methods. *Lane 1* plasmid DNA (1 μg), *lane 2* plasmid DNA + 10 μ*M* doxorubicin, *lane 3* plasmid DNA + 0.35 μg/ml TR, *lane 4* plasmid DNA + TR + 3.2 μ*M* Trx, *lane 5* plasmid DNA + TR + doxorubicin, *lane 6* plasmid DNA + TR + Trx + doxorubicin, *lane 7* plasmid DNA + TR + Trx + doxorubicin + SOD (2 U)

Superoxide generated by the Trx system with anthracyclines induces DNA damage in vitro

To further determine whether the $O_2^{\bullet-}$ generated by anthracyclines in the presence of the Trx system could cause damage to the DNA, we incubated closed circular plasmid DNA (pBL-CAT6, free of nicks) with the Trx system in the presence or absence of doxorubicin. As shown in Fig. 2, TR alone or the TR-Trx system in the presence of doxorubicin-induced nicks in the supercoiled DNA caused retarded migration in agarose electrophoresis (Fig. 2. lanes 5 and 6). The appearance of nicks in the plasmid DNA was higher in reactions containing Trx-TR than in those containing only TR (Fig. 2, lane 6). However, in the presence of SOD the extent of DNA nicking was inhibited (Fig. 2. lane 7), demonstrating that $O_2^{\bullet-}$ does mediate DNA damage due to redox-cycling of anthracyclines by the TR-Trx system. This result also indicates that the addition of Trx offers no protection from $O_2^{\bullet-}$-mediated damage to the plasmid DNA.

Oxidation of Trx during redox-cycling of anthracyclines is not inhibited by SOD

To evaluate the role of Trx in the process of redox-cycling of anthracyclines, we determined the redox state of Trx at the end of a redox-cycling reaction. If Trx-SH donates electrons for redox-cycling of anthracyclines

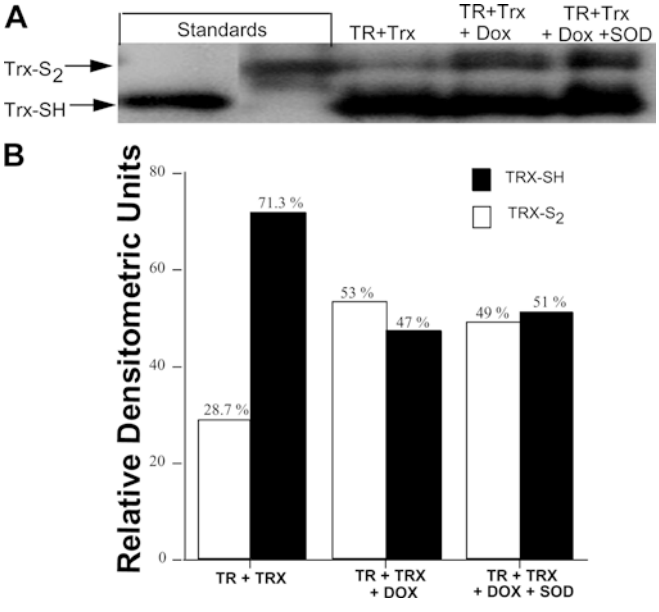

Fig. 3 **a** Redox state of Trx during redox-cycling of anthracyclines. Western blot detection of redox state of Trx after carboxymethylation and separation in native PAGE was performed as described in Materials and methods. *Lane 1 E. coli* Trx-SH standard (1 ng); *lane 2 E. coli* oxidized Trx standard; *lane 3* Trx redox state in the presence of *E. coli* Trx and TR; *lane 4* Trx redox state in the presence of Trx, TR and doxorubicin; *lane 5* Trx redox state in the presence of Trx, TR, doxorubicin and SOD. **b** Densitometric analysis of Western blots shown in Fig. 3a

then we would expect to find more oxidized Trx at the end of the reaction. Thus, as demonstrated in Fig. 3 (lane 4), the level of Trx-S_2 was increased in the presence of doxorubicin (28.7% with TR and NADPH to 53% with doxorubicin, TR and NADPH). Additionally, the level of reduced Trx decreased to 47% from 71.3% with the Trx-TR system only. SOD did not prevent oxidation of Trx in the presence of doxorubicin (Fig. 3b, lane 3). This suggests that the level of $O_2^{\bullet -}$ generated due to redox-cycling may not directly oxidize Trx.

Trx-SH donates electrons to CPR and enhances redox-cycling of doxorubicin

CPR is the principal enzyme that redox-cycles anthracyclines and uses NADPH as the source of reducing equivalents for this reaction [14]. Our observation that the Trx system could enhance the redox-cycling of anthracyclines prompted us to examine whether Trx-SH alone could be an electron donor for other flavoprotein enzyme such as CPR. The addition of 11.2 μ*M* Trx-SH induced CPR activity in the absence of NADPH, whereas the addition of 11.2 μ*M* Trx-S_2 did not result in any detectable CPR activity (Fig. 4a), indicating that CPR can accept electrons from Trx-SH. We further analyzed whether this activation of CPR was sufficient to catalyze the redox-cycling of doxorubicin. As shown in Fig. 4b (lane 4) CPR generated $O_2^{\bullet -}$ in the presence of 10 μ*M* doxorubicin and 11.2 μ*M* Trx-SH, but without NADPH (Fig. 4b). Thus, Trx-SH could substitute for NADPH as an electron donor for CPR. In similar reactions (Fig. 4b, lane 4) TR also redox-cycled doxorubicin using 11.2 μ*M* Trx-SH as an electron donor. However, Trx-SH was more efficient with CPR in the redox-cycling of doxorubicin than *E. coli* TR, since the concentrations of TR and CPR used in these assays were the same (10 n*M*).

Fig. 4 a Trx-SH donates electron to CPR. CPR activity was determined as described in Materials and methods. *Lane 1* blank, buffer, and cytochrome *c* only, *lane 2* 11.2 μ*M* Trx-SH and cytochrome P450 (10 n*M*), *lane 3* 11.2 μ*M* Trx-S_2 and cytochrome P450 (10 n*M*). **b** Trx-SH enhances redox-cycling of doxorubicin by donating electrons to CPR. Generation of superoxide was detected as reduction of SOD-inhibitable ferricytochrome *c* as described in Materials and methods. *Lane 1* 10 μ*M* doxorubicin + 11.2 μ*M* *E. coli* Trx-SH, *lane 2* CPR (0.04 U) + 11.2 μ*M* Trx-SH, *lane 3* CPR (0.04 U) + 11.2 μ*M* *E. coli* Trx-SH + doxorubicin (10 μ*M*), *lane 4* 0.35 μg TR, 10 μ*M* doxorubicin, and 11.2 μ*M* *E. coli* Trx-SH. *$P < 0.05$ vs blank and Trx-S_2 in Fig. 5a; $P < 0.05$ vs *lane 1* and *lane 2* in Fig. 5b

Externally added *E. coli* Trx increases ROS generation in response to doxorubicin in lung adenocarcinoma A549 cells

If *E. coli* Trx enhances $O_2^{\bullet -}$ generation due to redox-cycling of doxorubicin, we would expect that externally added Trx (if it could enter cells) would also increase ROS generation in response to anthracyclines. We have previously demonstrated that *E. coli* Trx can enter A549 lung adenocarcinoma cells [4]. *E. coli* Trx could act as a substrate for human TR, although its K_m is quite high (35 μ*M*) [15]. In addition, we have also previously reported that internalized *E. coli* Trx can be reduced within A549 cells [4]. Therefore, we sought to determine whether externally added *E. coli* Trx could enhance ROS production in response to anthracyclines. We incubated A549 cells with 32 μ*M* *E. coli* Trx for 16 h and determined the uptake of *E. coli* Trx by A549 cells by immunolocalization with an anti-*E. coli* Trx antibody. Confocal microscopy image scans obtained in *Z*-axis mode demonstrated that *E. coli* Trx entered the A549 cells and localized in the cytoplasm (Fig. 5b).

Next, we treated *E. coli* Trx-enriched A549 cells with or without 5 μ*M* doxorubicin. No ROS were detected in cells treated with only *E. coli* Trx (Fig. 6a). When cells were treated with doxorubicin, ROS generation was increased (Fig. 6b). However, when cells were pretreated with *E. coli* Trx followed by treatment with a 5 μ*M* doxorubicin, significantly higher levels of ROS generation were observed (Fig. 6c). The intensity of DCF-DA fluorescence was measured at specific times up to 300 s after the addition of drug in time-matched experiments,

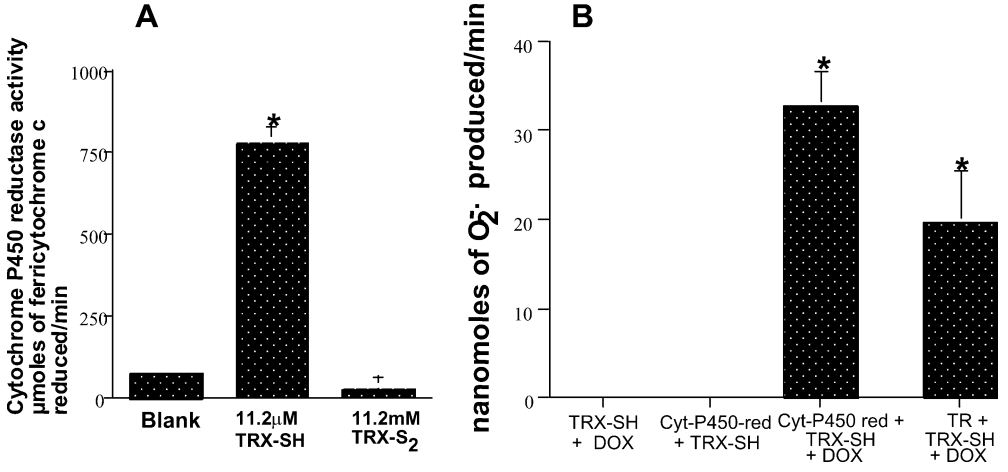

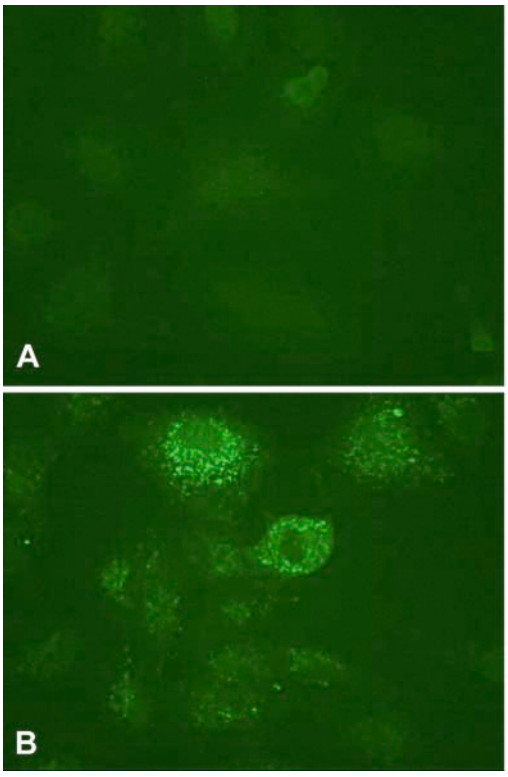

Fig. 5a, b Confocal microscopy of immunolocalization of *E. coli* Trx in A549 cells. A549 cells were incubated with or without *E. coli* Trx (32 μ*M*) for 16 h followed by detection of intracellular *E. coli* Trx using confocal microscopy as described in Materials and methods: **a** A549 cells without *E. coli* Trx; **b** A549 cells incubated with *E. coli* Trx (32 μ*M*, 16 h). Images represent mid sections of confocal laser scans showing bright green fluorescence indicating the presence of *E. coli* Trx in the cytoplasm of A549 cells

and the data plot (Fig. 6d) indicates higher mean fluorescence intensity of DCF-DA in A549 cells pretreated with *E. coli* Trx over the period of time compared to cells treated with doxorubicin alone. These results indicate that *E. coli* Trx could enhance the redox-cycling process of anthracyclines in human cells.

Increased TUNEL-positive nuclei in A549 cells treated with *E. coli* Trx in response to daunomycin

To determine whether the enhanced redox-cycling of anthracyclines in the presence of *E. coli* Trx could induce DNA strand breaks (nicks), A549 cells were incubated with *E. coli* Trx and treated with daunomycin for 4 h. Formation of DNA nicks in situ was detected using the TUNEL assay as described in Materials and methods. As shown in Fig. 7, A549 cells treated with *E. coli* Trx showed a significantly higher number of TUNEL-positive nuclei in response to daunomycin. Thus, it is evident that externally added *E. coli* Trx was able to enhance the redox-cycling of anthracyclines in vivo generating more strand breaks in the DNA.

Enhanced p53 DNA binding in response to daunomycin in A549 cells enriched with *E. coli* Trx

p53 is a sequence-specific transcription factor that is known to be activated in response to DNA damage [16], and DNA damage induced by anthracyclines is known to activate p53 DNA binding [16]. Therefore p53 DNA binding could be used as a marker for the extent of DNA damage induced by anthracyclines. As demonstrated in Fig. 8 increased p53 DNA binding was observed in daunomycin-treated A549 cells enriched with *E. coli* Trx. This finding shows that at low physiological doses of anthracyclines, *E. coli* Trx can increase DNA damage in vivo.

Discussion

In the present study we showed that anthracyclines could generate higher level of ROS in the presence of the Trx system. We also show that reduced Trx could act as an electron donor to other flavoprotein enzymes, such as CPR that catalyzes redox-cycling of anthracyclines. We demonstrated that *E. coli* Trx could increase the generation of ROS in the presence of anthracyclines resulting in increased DNA damage in A549 cells enriched with *E. coli* Trx. Taken together, these findings suggest that Trx could act as a pro-oxidant in the presence of anthracyclines resulting in increased ROS production. To the best of our knowledge there have been no previous studies demonstrating a pro-oxidant property of the Trx system.

Redox-cycling of anthracyclines begins with the formation of semiquinone radical and the subsequent generation of superoxide radical, both of which are necessary for the cytotoxic action of anthracyclines [17]. The redox-cycling of anthracyclines is extremely rapid and results in the formation of semiquinone DNA adducts and the generation of superoxide close to the DNA that causes more lethal damage to the DNA [18]. The primary role of bioreductive enzymes in the redox-cycling of anthracyclines is the reduction reaction catalyzing the formation of semiquinone radical. It is the semiquinone form that spontaneously reacts with oxygen to generate superoxide, which is proportional to the rate of formation of semiquinone. We demonstrated that the *E. coli* Trx-TR system could catalyze the redox-cycling of anthracyclines, and Trx could enhance this process. While several studies with TR derived from different species have demonstrated the role of TR in reducing quinones [19, 20] and generation of $O_2^{\bullet -}$ [21], our study showed that redox-cycling of anthracyclines by TR is enhanced in the presence of Trx and the superoxide generated due to redox-cycling is not inhibited by Trx. Therefore, Trx could act as a pro-oxidant molecule in the presence of anthracyclines.

We have previously shown that Trx is not able to scavenge superoxide anion generated by the xanthine–

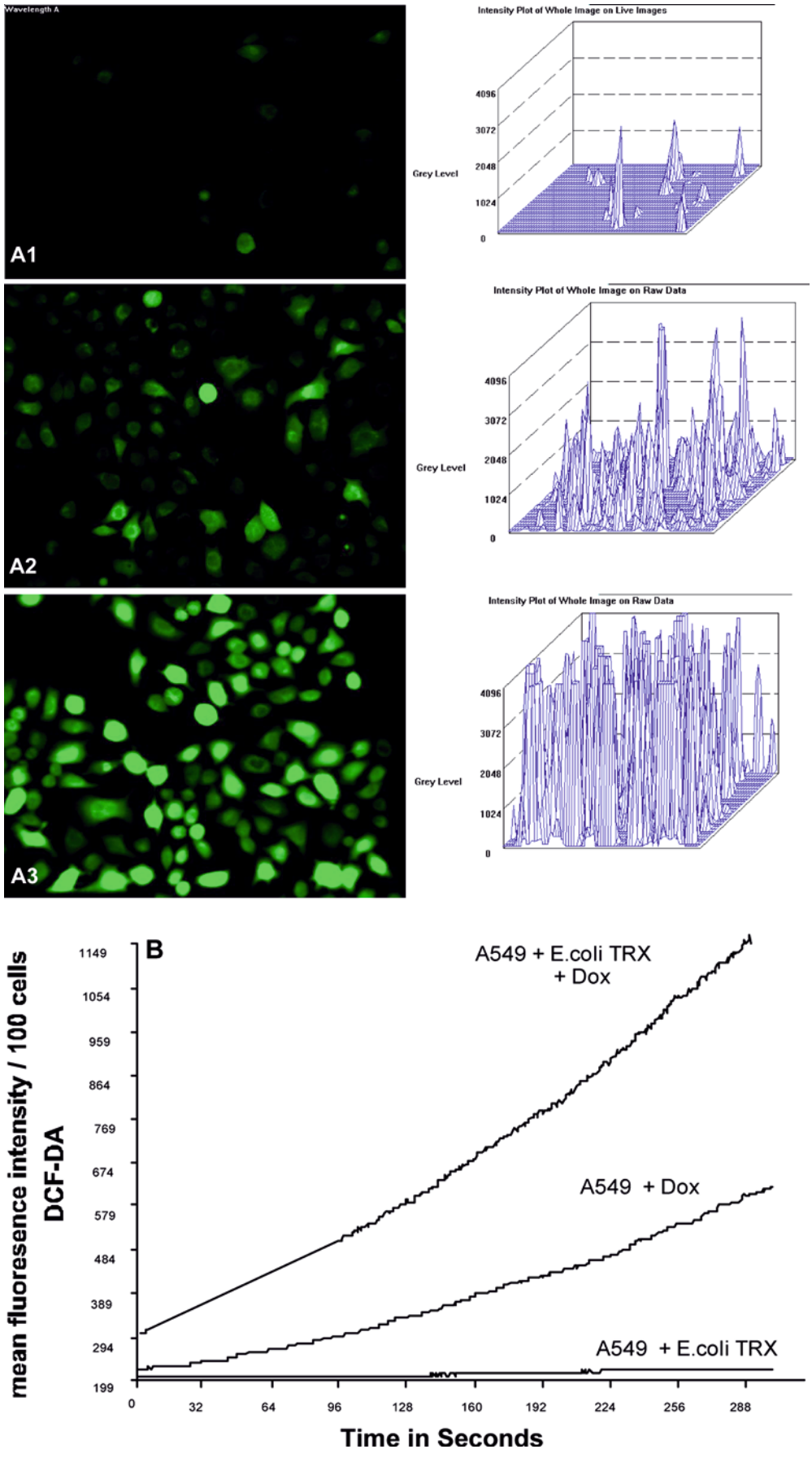

Fig. 6a, b Externally added *E. coli* Trx increases ROS generation in response to doxorubicin in A549 cells. A549 lung adenocarcinoma cells were incubated with *E. coli* Trx (16 h, 32 μ*M*). Cells were then incubated with 5 μ*M* doxorubicin, and DCF-DA fluorescence was measured using a laser confocal microscope. **a** Time-matched pictures taken at the 300th second: **a***1* A549 cells treated with *E. coli* Trx only; **a***2* A549 cells treated with doxorubicin only (5 μ*M*); **a***3* cells treated with *E. coli* Trx (32 μ*M*, 16 h) and doxorubicin (5 μ*M*). Enhanced green fluorescence demonstrates increased ROS formation. **b** Average DCF-DA fluorescence intensity of 100 cells in each experiment assayed in triplicate measured for a period of 300 s after the addition of doxorubicin

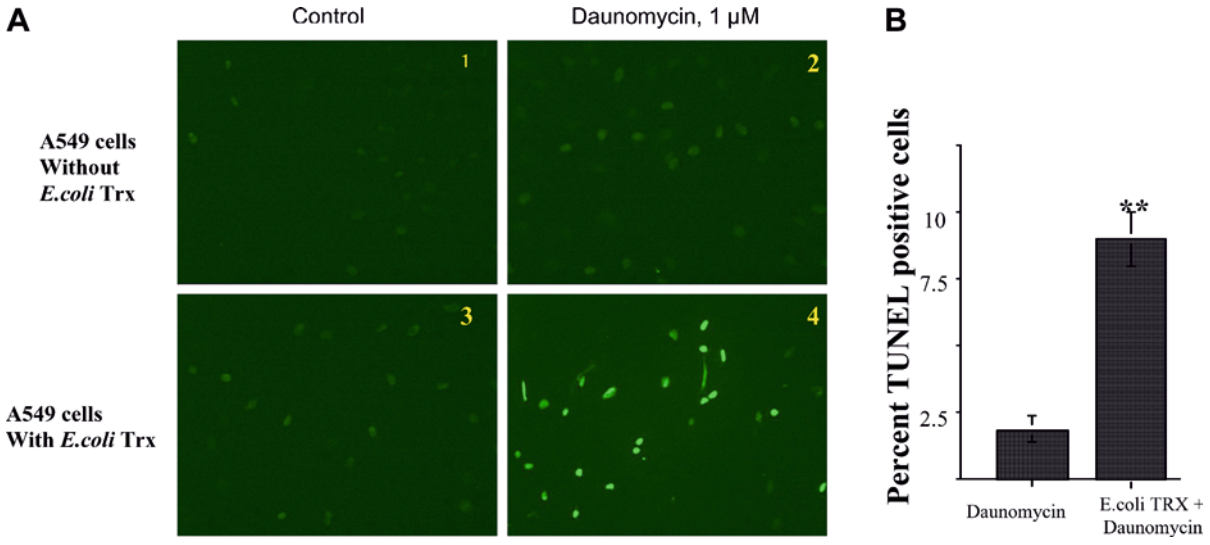

Fig. 7a, b Daunomycin in the presence of *E. coli* Trx induces DNA strand breaks in A549 cells. **a** *1* A549 cells, *2* A549 cells treated with daunomycin (1 μ*M*) for 4 h, *3* A549 cells treated with *E. coli* Trx (32 μ*M*) for 16 h, *4* A549 cells treated with *E. coli* Trx (32 μ*M*) for 16 h followed by daunomycin (1 μ*M*) for 4 h. The TUNEL assay was performed as described in the Materials and methods. TUNEL-positive nuclei were detected as green fluorescence on confocal microscopy. **b** Graph representing percent TUNEL-positive nuclei in cells treated with daunomycin (1 μ*M*) with or without *E. coli* Trx (32 μ*M*). **Significantly higher than cells treated with anthracycline only

xanthine oxidase system [5], which further supports the findings of the present study showing lack of inhibition of $O_2^{\bullet-}$ production by Trx during redox-cycling of anthracyclines. In addition, Trx did not protect against the formation of nicks in the plasmid DNA as compared with SOD (Fig. 2). Previous studies with *E. coli* Trx have shown that Trx is able to effectively reduce the drug alloxan while TR is unable to do so [22]. Therefore, we sought to determine whether Trx-SH could directly reduce anthracyclines. We did not detect any SOD-inhibitable $O_2^{\bullet-}$ generation with Trx-SH and anthracyclines in our assays (data not shown). Further, our Western blot detection of the redox status of Trx in these assays did show oxidation of Trx residues in the presence of SOD (Fig. 3) demonstrating that $O_2^{\bullet-}$ does not oxidize Trx, but Trx-S_2 accumulates due to transfer of electrons either to the quinone moiety of anthracycline or to TR, which remains to be elucidated. It is possible that oxidized Trx accumulates in the presence of TR and NADPH due to inactivation of TR by doxorubicin [19]. However, the $O_2^{\bullet-}$ production was linear during our assay period, indicating that TR remained active during our assay and incubation of TR with doxorubicin for extended periods has been shown to inactivate TR [19]. Based on previously published data, it is likely that *E. coli* TR may use Trx-SH as the source of electrons which can be transferred to other substrates [23], and also the efficiency of electron transfer by human TR to other substrates is enhanced by increasing the Trx concentration.

CPR is the principle drug-metabolizing enzyme, and efficiently redox-cycles anthracyclines [14]. We investigated the possible role of Trx-SH in CPR-mediated redox-cycling of anthracyclines. Our results (Fig. 4a) show that CPR is activated by Trx-SH in the absence of NADPH. In contrast, Trx-S_2 did not activate CPR. We further investigated whether Trx-SH would also enhance the redox-cycling of anthracyclines by CPR. Our results (Fig. 4b) demonstrate that Trx-SH was able to enhance the redox-cycling of anthracyclines by CPR as well. The efficiency of the redox-cycling of doxorubicin by CPR was higher than equimolar concentrations of *E. coli* TR using Trx-SH as the source of electrons.

Our in vivo studies with A549 cells enriched with *E. coli* Trx demonstrated increased ROS production and DNA strand breaks in the presence of anthracyclines. Based on p53 DNA binding, at lower drug concentrations, *E. coli* Trx was able to enhance DNA damage (Figs. 7 and 8). Since p53 is implicated in growth arrest,

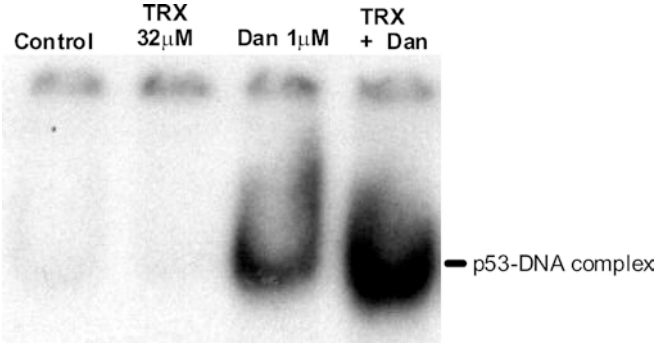

Fig. 8 Enhanced p53 DNA binding in *E. coli* Trx-enriched A549 cells in response to daunomycin. A549 cells were incubated with 32 μ*M* *E. coli* Trx for 16 h. Following incubation cells were treated with daunomycin (1 μ*M*) for 4 h, nuclear extract was prepared and EMSA was performed as described in Materials and methods. *Lane 1* control A549 cells, *lane 2* cells incubated with 32 μ*M* *E. coli* Trx (16 h), *lane 3* cells treated with 1 μ*M* daunomycin, *lane 4* cells incubated with *E. coli* Trx followed by treatment with 1 μ*M* daunomycin

DNA repair and apoptosis [24], our future goal is to elucidate the consequences of DNA damage and enhanced p53 DNA binding induced by anthracyclines in the presence of *E. coli* Trx in terms of cellular response to cytotoxic drug therapy.

In summary, the present study demonstrated a novel role of Trx in redox-cycling of anthracyclines. Although, Trx has been shown to possess potent antioxidant properties [5], it could also enhance the generation of $O_2^{\bullet -}$ due to redox-cycling of anthracyclines, which is critical to the cytotoxic action of anthracyclines.

Acknowledgments This study was supported by a research project grant from the American Cancer Society (K.C.D.), and from NIH (1 R0 HL071558).

References

1. Powis G, Briehl M, Oblong J (1995) Redox signaling and the control of cell growth and death. Pharmacol Ther 68:149–173
2. Lundstrom J, Holmgren A (1990) Protein disulfide-isomerase is a substrate for thioredoxin reductase and has thioredoxin-like activity. J Biol Chem 265:9114–9120
3. Fernando MR, Nanri H, Yoshitake S, Nagata-Kuno K, Minakami S (1992) Thioredoxin regenerates proteins inactivated by oxidative stress in endothelial cells. Eur J Biochem 209:917–922
4. Das KC, Lewis-Molock Y, White CW (1997) Elevation of manganese superoxide dismutase gene expression by thioredoxin. Am J Respir Cell Mol Biol 17:713–726
5. Das KC, Das CK (2000) Thioredoxin, a singlet oxygen quencher and hydroxyl radical scavenger: redox independent functions. Biochem Biophys Res Commun 277:443–447
6. Tanaka T, Nakamura H, Nishiyama A, Hosoi F, Masutani H, Wada H, Yodoi J (2001) Redox regulation by thioredoxin superfamily: protection against oxidative stress and aging. Free Radic Res 33:851–855
7. Mau BL, Powis G (1990) Inhibition of thioredoxin reductase (E.C. 1.6.4.5.) by antitumor quinones. Free Radic Res Commun 8:365–372
8. Berggren MI, Husbeck B, Samulitis B, Baker AF, Gallegos A, Powis G (2001) Thioredoxin peroxidase-1 (peroxiredoxin-1) is increased in thioredoxin-1 transfected cells and results in enhanced protection against apoptosis caused by hydrogen peroxide but not by other agents including dexamethasone, etoposide, and doxorubicin. Arch Biochem Biophys 392:103–109
9. Hrdina R, Gersl V, Klimtova I, Simunek T, Machackova J, Adamcova M (2000) Anthracycline-induced cardiotoxicity. Acta Medica (Hradec Kralove) 43:75–82
10. Yonetani T (1965) Studies on cytochrome c peroxidase. II. Stoichiometry between enzyme, H2O2, and ferrocytochrome c and enzymic determination of extinction coefficients of cytochrome c. J Biol Chem 240:4509–4514
11. Holmgren A, Reichard P (1967) Thioredoxin 2: cleavage with cyanogen bromide. Eur J Biochem 2:187–196
12. Das KC, Misra HP (1992) Antiarrhythmic agents. Scavengers of hydroxyl radicals and inhibitors of NADPH-dependent lipid peroxidation in bovine lung microsomes. J Biol Chem 267:19172–19178
13. Das KC (2001) c-Jun NH2-terminal kinase-mediated redox-dependent degradation of IkappaB: role of thioredoxin in NF-kappaB activation. J Biol Chem 276:4662–4670
14. Berlin V, Haseltine WA (1981) Reduction of adriamycin to a semiquinone-free radical by NADPH cytochrome P-450 reductase produces DNA cleavage in a reaction mediated by molecular oxygen. J Biol Chem 256:4747–4756
15. Luthman M, Holmgren A (1982) Rat liver thioredoxin and thioredoxin reductase: purification and characterization. Biochemistry 21:6628–6633
16. Tishler RB, Calderwood SK, Coleman CN, Price BD (1993) Increases in sequence specific DNA binding by p53 following treatment with chemotherapeutic and DNA damaging agents. Cancer Res 53:2212–2216
17. Taatjes DJ, Gaudiano G, Resing K, Koch TH (1997) Redox pathway leading to the alkylation of DNA by the anthracycline, antitumor drugs adriamycin and daunomycin. J Med Chem 40:1276–1286
18. Qu X, Wan C, Becker HC, Zhong D, Zewail AH (2001) The anticancer drug-DNA complex: femtosecond primary dynamics for anthracycline antibiotics function. Proc Natl Acad Sci U S A 98:14212–14217
19. Mau BL, Powis G (1992) Mechanism-based inhibition of thioredoxin reductase by antitumor quinoid compounds. Biochem Pharmacol 43:1613–1620
20. Bironaite D, Anusevicius Z, Jacquot JP, Cenas N (1998) Interaction of quinones with Arabidopsis thaliana thioredoxin reductase. Biochim Biophys Acta 1383:82–92
21. Nordberg J, Zhong L, Holmgren A, Arner ES (1998) Mammalian thioredoxin reductase is irreversibly inhibited by dinitrohalobenzenes by alkylation of both the redox active selenocysteine and its neighboring cysteine residue. J Biol Chem 273:10835–10842
22. Holmgren A, Lyckeborg C (1980) Enzymatic reduction of alloxan by thioredoxin and NADPH-thioredoxin reductase. Proc Natl Acad Sci U S A 77:5149–5152
23. Berglund O, Holmgren A (1975) Thioredoxin reductase-mediated hydrogen transfer from Escherichia coli thioredoxin-(SH)2 to phage T4 thioredoxin-S2. J Biol Chem 250:2778–2782
24. Sidransky D, Hollstein M (1996) Clinical implications of the p53 gene. Annu Rev Med 47:285–301